Air-Stable Blue Phosphorescent Tetradentate Platinum(II) Complexes as Strong Photo-Reductant

Kai Li, Qingyun Wan, Chen Yang, Xiao-Yong Chang, Kam-Hung Low, and Chi-Ming Che*

Abstract: *Strong photo-reductants have demonstrated important applications in photo-redox organic synthesis involving reductive activation of C-X(halide) and C=O bonds. We report herein air-stable Pt(II) complexes supported by tetradentate bis(phenolate-NHC) ligands having peripheral electron-donating N-carbazolyl groups. Photo-physical, electrochemical, and computational studies reveal that the presence of N-carbazolyl groups enhances the light absorption and redox reversibility because of its involvement into the frontier MOs in both ground and excited states, rendering the complexes robust strong photo-reductant with* $E([Pt]^{+/*})$ *over -2.6 V vs* $Cp_2Fe^{+/0}$. *The one-electron reduced [Pt]⁻ species are stronger reductants with* $E_{PC}([Pt]^{0/-})$ *up to -3.1 V vs* $Cp_2Fe^{+/0}$. *By virtue of the strong reducing nature of these species generated upon light excitation, these Pt(II) complexes can be used in light-driven reductive coupling of carbonyl compounds and reductive debromination of a wide range of unactivated aryl bromides.*

Strong photo-reductants have appealing applications in reductive C-C bond formation reactions that involve radical/radical ion intermediates, and which are usually accomplished under harsh conditions in ground state.[1] As depicted in Scheme 1, the substrate scope for light-induced single-electron transfer (SET) process is confined by ground state and excited state redox potentials of the photo-catalyst (**PC**), i.e. $E([\mathbf{PC}]^{+/*})$ and $E([\mathbf{PC}]^{0/-})$.[2,3] For the widely used photo-reductant $[Ir(ppy)_3]$, its $E([\mathbf{PC}]^{+/*})$ is -1.73 V vs SCE. Despite the $E([\mathbf{PC}]^{0/-})$ of -2.19 V, access to $[Ir(ppy)_3]^-$ is disfavored by the low excited state reduction potential for $E([\mathbf{PC}]^{*/-})$. In this context, a few organic dyes have proven to be strong photo-reductants.[4] By elegant design of consecutive photo-induced electron transfer, triplet-triplet annihilation (TTA) based up-conversion, or triplet sensitization/electron transfer processes, visible light can be used to generate strongly reducing species.[4a,c-e] It is noted that multi-component system is challenging to design because of the presence of multiple, plausible energy/electron transfer processes.[5] Therefore, the search for new powerful photo-reductant remains a crucial step to the development of new photo-redox catalysis for synthetic chemistry in terms of expanding substrates and for devising new reactions of synthetic interest.

As up to now, a few metal complexes of Cu(I),[6] W(0),[7] Mo(0),[8] and Cr(0)[9] have been shown to display strongly reducing excited states. But these complexes also have low redox potentials of ca. -(0.38–0.72) V vs $Cp_2Fe^{+/0}$ for the $M^{+/0}$ couple (Scheme 1), which disfavors regeneration of the metal complexes through reduction of their oxidized forms with common sacrificial electron donors, e.g. tertiary amines. Moreover, the air-sensitivity of the low-valent complexes may hamper their practical use.

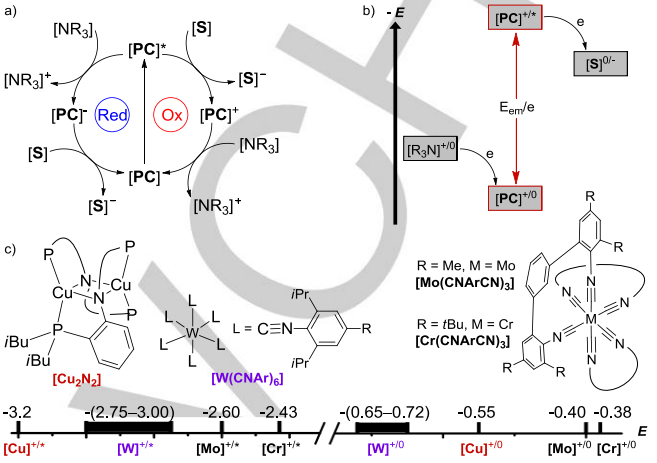

Scheme 1. (a) Two pathways for photo-reduction reactions. (b) Correlation among ground state and excited state redox potentials and emission energy. **PC**: photo-catalyst; **S**: organic substrate. (c) Structures of literature-reported complexes having strongly reducing excited states (potentials: V vs $Cp_2Fe^{+/0}$).

We propose to develop strong photo-reductants with blue phosphorescent tetradentate platinum(II) complexes[10] for the following reasons. First, the high energy (E_{em}) and tens of microseconds lifetime of the triplet excited states of blue phosphorescent metal complexes are instrumental to achieve strongly reducing excited state species (**[PC]***) for efficient bimolecular photochemical reactions. Second, the strong chelate effect of tetradentate ligand scaffold renders the platinum photo-catalyst robust against demetalation both in the ground and excited states. Third, Pt(II) complexes with open coordination sites may activate chemical bonds via inner-sphere atom transfer process. In this work, we chose Pt(II) complexes supported by the bis(phenolate-NHC) ligands bearing electron-donating *N*-carbazolyl groups (**1** and **2**, Figure 1). The analogue bearing strong electron-withdrawing CF_3 (**3**) and the other complexes, [Pt(ppy)(acac)], [Pt(pim)(acac)] and $[Ir(ppy)_3]$ were studied for comparison.

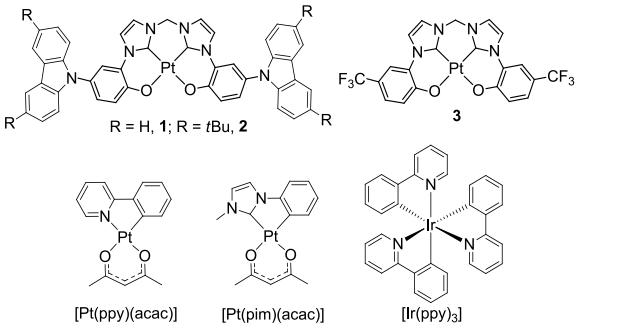

Figure 1. Chemical structures of Pt(II) complexes **1**–**3** and reference complexes.

Synthetic route (Scheme S1) and characterization data (multinuclear NMR and high-resolution mass spectra and elemental analyses) of **1**–**3** are given in the Supporting Information. Complexes **1**–**3** were prepared in 58–89% yields by a convenient reaction of $[Pt(DMSO)_2Cl_2]$ with bis(imidazolium) salts (synthesized from commercially available inexpensive materials). X-ray single crystal structures of **1** and **2** have been determined.[11] In both crystal structures, the peripheral carbazolyl groups are significantly twisted with respect to the phenolate plane. The

[*] Dr. K. Li, Q. Wan, Dr. C. Yang, Dr. X.-Y. Chang, Dr. K.-H. Low, Prof. Dr. C.-M. Che
State Key Laboratory of Synthetic Chemistry, Institute of Molecular Functional Materials, HKU-CAS Joint Laboratory on New Materials, and Department of Chemistry, The University of Hong Kong, Pokfulam Road, Hong Kong (China)
E-mail: cmche@hku.hk

Prof. Dr. C.-M. Che
HKU Shenzhen Institute of Research and Innovation, Shenzhen 518053 (China)

Supporting information for this article is given via a link at the end of the document.

crystal structure of **2** shows a roughly planar molecular backbone with a Pt···Pt and π-π contact of ~3.5 Å in each pair of molecules (Figure 2). In contrast, a bent conformation and a much shorter Pt···Pt distance of ~3.1 Å are observed in the crystal structure of **1** (Figure S1). The complexes are well soluble in DMF, but poorly soluble in MeCN and alcohol. DMF was selected as the solvent for the electrochemical, photo-physical and photochemical studies. The photo-stability of **2** in degassed solution was examined (Figure 3). Continuous irradiation of a [D_7]DMF solution of **2** using a UV lamp (365 nm, 12 W) for 96 h in the absence of oxygen did not induce notable change.

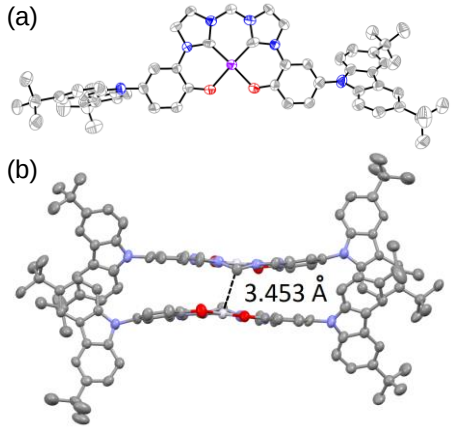

Figure 2. Crystal structure of **2**. (a) Top view. (b) Side view.

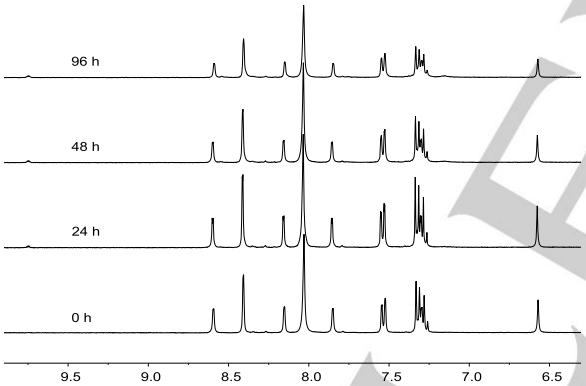

Figure 3. ^{1}H NMR spectral traces of **2** in degassed [D_7]DMF upon UV lamp irradiation (365 nm, 12 W).

Complexes **1**–**3** exhibit intense absorptions in DMF in UVA region (λ = 315–400 nm) (Table 1, Figure 4a, and Figure S2) with ε on the order of 10^4 M^{-1} cm^{-1}. With respect to previous studies,[10a,b] the lowest-energy absorptions are assigned to mixed π(phenolate)→π*(NHC) (^{1}ILCT) and dπ(Pt)→π*(NHC) (^{1}MLCT) transitions. Notably, the presence of *N*-carbazolyl groups results in increased molecular absorptivity for **1** and **2** in the lowest-energy ^{1}ILCT/^{1}MLCT transitions compared to that of **3**, revealing the involvement of carbazolyl groups in the transition. A blue shift of ca. 20 nm was observed for **3** relative to **1** and **2**, likely due to the stabilization of HOMO level arising from strong electron-withdrawing effect of CF_3. Solvatochromic study for **2** reveals a slight blue shift of the lowest energy absorption maximum by 4 nm upon changing the solvent from toluene (λ_{max} = 368 nm) to DMF (λ_{max} = 364 nm) (Figure S2). Absorption from $S_0 \rightarrow T_1$ transition has not been located. Complexes **1** and **2** display strong blue emission in solutions and in PMMA films at room temperature (Figure 4a and Figure S2), which are assigned to be predominantly from the triplet π(phenolate/carbazole)-π*(NHC) (^{3}ILCT) excited states perturbed by the Pt(II) center. The PLQYs (Φ) of **2** in toluene and PMMA (5 wt%) reach 40%. In sharp contrast, **3** shows the highest emission energy but with a very low Φ value (1% in DMF). A thermally accessible non-radiative state is likely the reason. The emission properties of **1**–**3** in other states are provided in the Supporting Information (Table S2 and Figure S3).

Table 1: Photo-physical data of **1**–**3** in DMF at room temperature.

	Absorption[a] λ_{max} / nm (ε / 10^4 M^{-1} cm^{-1})	Emission[a,b] λ_{max} / nm (τ / μs); Φ
1	284 (4.79), 308 (sh, 1.88), 345 (2.14), 359 (1.92)	446 (6.1); 20%
2	288 (4.87), 298 (5.08), 352 (2.17), 364 (1.78)	447 (6.7); 24%
3	274 (sh, 2.50), 291 (1.60), 332 (1.35), 345 (1.50)	434 (0.16); 1%

[a] In DMF (concentration ~2 × 10^{-5} M). [b] λ_{ex} = 350 nm (**1** and **2**) or 345 nm (**3**).

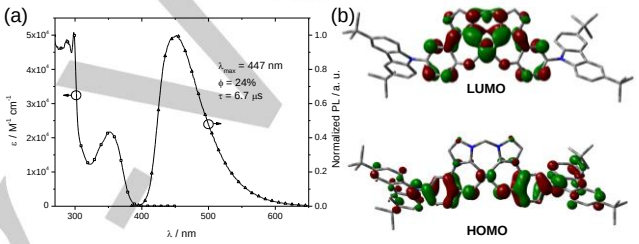

Figure 4. (a) UV/Vis absorption and emission spectra of **2** in DMF at room temperature; concentration ~ 2 × 10^{-5} M. (b) DFT calculated HOMO and LUMO of **2** in S_0 state.

Table 2: Rate constants for the quenching of **2*** (λ_{ex} = 350 nm) by various organic substrates (**S**) in DMF at room temperature.

	$E(S^{0/-})$ / V vs SCE	k_q / M^{-1} s^{-1}
Acetophenone	-2.14[a]	1.33 × 10^9
Benzaldehyde	-1.81[a]	2.53 × 10^9
4-Chlorobenzonitrile	-2.03[a]	1.88 × 10^8
Benzonitrile	-2.31[a]	2.71 × 10^6
Chloroform	-2.35[b]	2.18 × 10^7
Benzyl chloride	-2.21[b]	1.47 × 10^7
2-Chlorobromobenzene	-2.78[b]	4.30 × 10^6
4-Fluorobromobenzene	-2.66[b]	4.96 × 10^5

[a] Half reduction potential. [b] Cathodic peak potential.

DFT and TDDFT calculations were performed on **1** and **2** as well as **Pt-H** to decipher the effect of *N*-carbazolyl groups on their electronic structures (Figure 4b and Figures S4–S6). In the S_0 state, the electron density of HOMO for **1** and **2** distributes over the N atoms of carbazolyl groups and the phenolate moieties, in comparison to that for analogue **Pt-H**. The increased oscillator strength for **1** and **2** is also reproduced from calculations (Figure S7). Unexpectedly, the calculations show that **1** and **2** undergo different $S_0 \rightarrow T_1$ excited state geometry distortions and the frontier MOs of **1** and **2** in T_1 state have different contour plots. As for **Pt-H** and previous reported complexes, the NHC ring that dominantly contributes to the SOMO is twisted in T_1 state for **1**. Meanwhile, the *N*-carbazolyl group rotates by ~14° to have a smaller torsion angle with the phenolate ring, due to the decrease of electron density on N atom upon photo-excitation. In contrast, the substitution of *t*Bu groups results in the T_1 state of **2** to have mainly π(*t*Bu-carbazole$_1$ + phenolate)→π*(*t*Bu-carbazole$_2$) charge-transfer character. As a result, NHC twisting has not been observed in the calculation. In view of their quite similar absorption and emission properties in solutions, it might not be appropriate to assign the T_1 states of **1** and **2** to

be different. Instead, the T_1 states of **1** and **2** are assigned tentatively to have π(*t*Bu-carbazole$_1$ + phenolate)→π*(*t*Bu-carbazole$_2$ + NHC) charge-transfer character with varying degree of each components.

Electrochemical studies by cyclic voltammetry revealed that **2** and **3** show oxidation waves at 0.35 V and 0.50 V (E_{pa}) vs $Cp_2Fe^{+/0}$, respectively (Figure 5). Notably, this oxidation process is more reversible for **2** than for **3**, presumably due to the contribution from carbazoyl groups to HOMO in **2**. From the Latimer diagram, the excited-state redox potential $E([Pt]^{+/*})$ of **2** is estimated to be -2.63 V vs $Cp_2Fe^{+/0}$, revealing that the excited state reducing power is comparable to those of the most powerful photo-reductants of W(0),[7] Mo(0)[8] and organic dye.[4] It is noted that the one-electron reduced species $[Pt]^-$ (for **2**) with $E([Pt]^{0/-})$ of -3.05 V vs $Cp_2Fe^{+/0}$ is a stronger reductant. For **3**, the CF_3 substitution has no appreciable effect on the potential of the reduction peak. Previously reported **Pt-F** and **Pt-Me**[10b] were also studied for comparison. Complex **Pt-F** shows similar $E([Pt]^{+/*})$ and $E([Pt]^{0/-})$ values as **2** while **Pt-Me** shows a more cathodic $E([Pt]^{0/-})$ wave (Figure S8). Therefore, the reduction potentials of both [Pt]* and $[Pt]^-$ for **3** and **Pt-F** are virtually the same as those of **2** (Figure S8). The strong absorption, long emission lifetime, and increased redox reversibility of **2** suggest that it is a promising, strong photo-reductant.

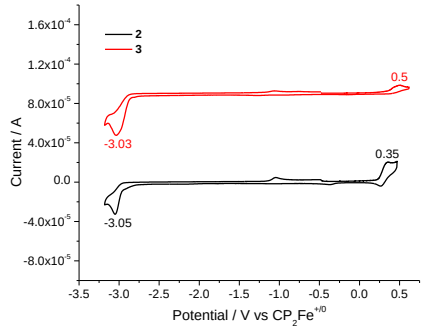

Figure 5. Cyclic voltammograms of **2** and **3** in DMF.

The redox properties of **2*** were first examined through Stern-Volmer experiments with a panel of pyridinium salts having reduction potentials ($E_{1/2}$) from -0.67 to -1.68 V *vs* SCE. The diffusion-corrected quenching rate constants are close to diffusion controlled limit, being in the range of 1.81–5.17 × 10^9 s^{-1} (Figure S9 and Table S3). The strong reducing power of **2*** is also revealed by its emission being quenched by aryl carbonyls with rate constants on the order of 10^9 M^{-1} s^{-1} (Table 2 and Figures S10−S11). The emission of **2** is quenched by benzonitrile (Table 2 and Figure S10) with a relatively low quenching rate constant; presumably, the excited state reduction potential of **2** is close to the reduction potential of benzonitrile at -2.76 V vs $Cp_2Fe^{+/0}$. This is in agreement with the estimated value of -2.63 V for **2** from electrochemical and spectroscopic measurements. Importantly, the emission of **2** can be quenched by diisopropylethylamine (DIPEA) (Figure S12) with a rate constant of 3.71 × 10^5 M^{-1} s^{-1}, revealing the possibility to generate $[\mathbf{2}]^-$ that can act as a stronger reductant.

The light-induced reductive coupling of carbonyl compounds with **2** as catalyst was examined. With DIPEA as sacrificial electron donor, a panel of aromatic carbonyls underwent pinacol coupling reaction to afford diols in yields of 65−91% (Table 3 and Table S4). Control experiments (Table S5) confirmed the essential roles of Pt(II) catalyst, DIPEA, and light for this process. Unlike the cases where amine cations or external additives are required to activate carbonyl groups,[3e,f] the substrates in this work are proposed to be reduced directly by **2***; this is also revealed by the large oxidative quenching rate constants depicted in Table 2. When **3** or **Pt-Me** was used, lower yields (< 40%) were obtained for acetophenone, probably due to the weaker light absorption and/or the very short excited state lifetime; **Pt-F** gave a higher yield than **3** and **Pt-Me**; the use of [Pt(ppy)(acac)], [Pt(pim)(acac)], or [Ir(ppy)$_3$] resulted in low yields of 9−18% (Table S5). A plausible reaction pathway is proposed in Scheme S2.

Table 3: Light-driven reductive coupling of aromatic carbonyls.[a,b]

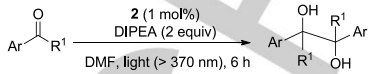

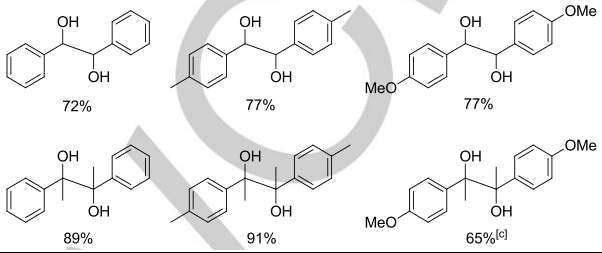

[a] Reaction conditions: Aromatic carbonyl (0.2 mmol), catalyst (1 mol%), DIPEA (0.4 mmol), DMF (2 mL), xenon lamp (λ > 370 nm). [b] Product yield determined by ^{1}H NMR spectroscopy using an internal standard. [c] Reaction time of 24 h.

Reductive radical dehalogenation that avoids the use of toxic organotin reagent is a useful tool in organic synthesis.[12] Photo-redox catalysis via electron transfer provides an appealing approach to the generation of radical anions because of the mild reaction conditions and good functional group tolerance. However, examples of photo-catalysts that are able to reduce unactivated alkyl and aryl bromides upon light irradiation are sparse.[2c,4] We examined the applicability of **2** for reductive debromination of unactivated aryl bromides. With reference to the protocol reported by Stephenson and co-workers,[2b] in the presence of **2** (1.5 mol%), DIPEA (5 equiv), and formic acid (10 equiv) in DMF, **4a** was completely reduced to give **5a** in 96% yield after 4 h of irradiation with UVA LED (365 nm, 4.5 W). Control experiments showed that Pt(II) catalyst, DIPEA, and light are all essential for this transformation (Table S6). The presence of formic acid can improve the reaction. A range of Ar-Br bearing steric bulky (**4d**) and strongly electron-donating (**4h**,**i**) substituents were converted to Ar-H in good yields (74−81%, Table 4). Carboxyl, hydroxyl, and amide groups can be tolerated in this transformation as well in reasonable yields (**4j**−**l**). For reduction of **4a**, the use of **3**, **Pt-F**, or **Pt-Me** gave **5a** in 46−61% yields under the same reaction conditions; [Pt(ppy)(acac)] or [Pt(pim)(acac)] resulted in low yields of 9−16% (Table S6). The reduction potential of [Pt(ppy)(acac)] ($E([Pt]^{+/*})$ = -2.07 V *vs* SCE) is insufficient to reduce unactivated Ar-Br.[2g] In spite of a high emission energy, the short triplet excited state lifetime of [Pt(pim)(acac)] is postulated to render a low catalytic efficiency.[13] [Ir(ppy)$_3$] was found to be ineffective for the photochemical reduction of **4a** under the same conditions.

Previous works on photo-redox catalyzed debromination pointed to radical mechanism. A few alkyl and arylbromides **4m**−**p** were subjected to the reaction conditions and found to undergo cyclization to afford products in moderate to excellent yields (Scheme S3), substantiating the radical mechanism.[14] Intermolecular radical-radical coupling was also demonstrated on benzyl chloride (**4q**) to furnish the desired homocoupled product (Scheme S4). The Pt(II) complexes may activate halocarbons via outer-sphere electron transfer and/or inner-sphere atom abstraction processes. Photoreactions of **2** with a series of organic halides were investigated by Stern-Volmer quenching studies. The rate constants for the quenching of emission of **2** are found to depend on the reduction

potential rather than the bond dissociation energy of the R-X substrates (Table 2 and Figure S13). For example, k_q of 4-chlorobenzonitrile (1.88 × 10^8 M^{-1} s^{-1}) is much faster than that for a variety of alky and aryl bromides. Thus, the quenching is mainly attributed to outer-sphere electron transfer from ***2**** to R-X. Based upon the emission quenching experiments with R-Br and DIPEA, a plausible reaction mechanism involving both oxidative and reductive processes is proposed (Scheme S5).

Table 4: Light-driven reductive hydrodebromination of aryl bromides.[a,b]

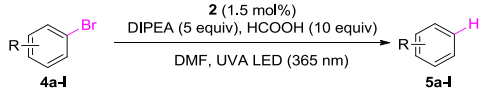

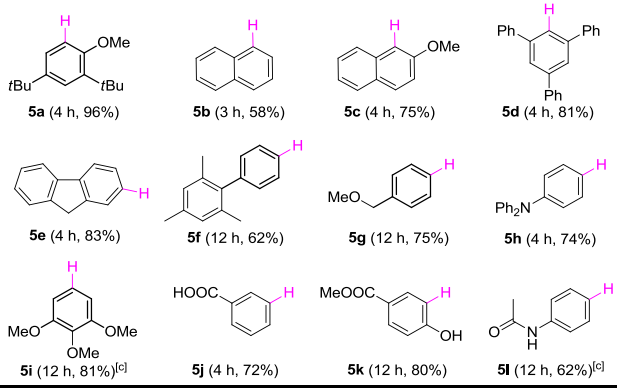

[a] Reaction conditions: substrate (0.1 mmol), **2** (1.5–5 mol%), DIPEA (0.5 mmol), formic acid (40 µL), and UVA LED (365 nm, 4.5 W). [b] Product yield determined by ^{1}H NMR spectroscopy using an internal standard. [c] 5 mol% **2** used.

In summary, strongly electron-donating carbazolyl groups have been incorporated into blue phosphorescent Pt(II) complexes supported by tetradentate bis(phenolate-NHC) ligands to develop air-stable strong photo-reductants. The Pt(II) complex displays strong excited state reducing ability with $E([Pt]^{+/*})$ over -2.6 V vs $Cp_2Fe^{+/0}$. The one-electron reduced species is stronger reductant with $E_{pc}([Pt]^{+/0})$ at -3.1 V vs $Cp_2Fe^{+/0}$. Together with long excited state lifetime, the complex is able to drive light-induced reductive coupling of aromatic carbonyl compounds and reductive debromination of unactivated aryl bromides in good to excellent yields under mild conditions. This work highlights that Pt(II) complexes supported by tetradentate ligands are promising robust photo-catalysts for organic synthesis.

Acknowledgements

This work was supported by the National Key Basic Research Program of China (No. 2013CB834802), the Hong Kong Research Grants Council (HKU17330416), the University Grants Committee Areas of Excellence Scheme (AoE/P-03/08), CAS-Croucher Foundation Funding Scheme for Joint Laboratories, and the Science and Technology Innovation Commission of Shenzhen Municipality (JCYJ20160530184056496).

Keywords: photo-redox catalysis • photo-reductant • Pt(II) complex• radical dehalogenation • C-C bond formation

[1] Selected reviews: a) J. M. R. Narayanam, C. R. J. Stephenson, *Chem. Soc. Rev.* **2011**, *40*, 102; b) C. K. Prier, D. A. Rankic, D. W. C. MacMillan, *Chem. Rev.* **2013**, *113*, 5322; c) D. M. Schultz, T. P. Yoon, *Science* **2014**, *343*, 1239176; d) D. Ravelli, S. Protti, M. Fagnoni, *Chem. Rev.* **2016**, *116*, 9850; e) I. Ghosh, L. Marzo, A. Das, R. Shaikh, B. König, *Acc. Chem. Res.* **2016**, *49*, 1566; f) M. Majek, A. Jacobi von Wangelin, *Acc. Chem. Res.* **2016**, *49*, 2316; g) J. Xie, H. Jin, A. S. K. Hashmi, *Chem. Soc. Rev.* **2017**, *46*, 5193.

[2] Selected examples: a) H. Kim, C. Lee, *Angew. Chem. Int. Ed.* **2012**, *51*, 12303; *Angew. Chem.* **2012**, *124*, 12469; b) J. D. Nguyen, E. M. D'Amato, J. M. R. Narayanam, C. R. J. Stephenson, *Nat Chem* **2012**, *4*, 854; c) G. Revol, T. McCallum, M. Morin, F. Gagosz, L. Barriault, *Angew. Chem. Int. Ed.* **2013**, *52*, 13342; *Angew. Chem.* **2013**, *125*, 13584; d) H. Huo, X. Shen, C. Wang, L. Zhang, P. Röse, L.-A. Chen, K. Harms, M. Marsch, G. Hilt, E. Meggers, *Nature* **2014**, *515*, 100; e) J. Xie, S. Shi, T. Zhang, N. Mehrkens, M. Rudolph, A. S. K. Hashmi, *Angew. Chem. Int. Ed.* **2015**, *54*, 6046; *Angew. Chem.* **2015**, *127*, 6144; f) M. Knorn, T. Rawner, R. Czerwieniec, O. Reiser, *ACS Catalysis* **2015**, *5*, 5186; g) W. J. Choi, S. Choi, K. Ohkubo, S. Fukuzumi, E. J. Cho, Y. You, *Chem. Sci.* **2015**, *6*, 1454; h) P.-K. Chow, G. Cheng, G. S. M. Tong, W.-P. To, W.-L. Kwong, K.-H. Low, C.-C. Kwok, C. Ma, C.-M. Che, *Angew. Chem. Int. Ed.* **2015**, *54*, 2084; *Angew. Chem.* **2015**, *127*, 2112; i) J.-J. Zhong, C. Yang, X.-Y. Chang, C. Zou, W. Lu, C.-M. Che, *Chem. Commun.* **2017**, *53*, 8948; j) R. Naumann, F. Lehmann, M. Goez, *Angew. Chem. Int. Ed.* **2018**, *57*, 1078; *Angew. Chem.* **2018**, *130*, 1090.

[3] Selected examples: a) F. R. Petronijević, M. Nappi, D. W. C. MacMillan, *J. Am. Chem. Soc.* **2013**, *135*, 18323; b) F. J. R. Klauck, M. J. James, F. Glorius, *Angew. Chem. Int. Ed.* **2017**, *56*, 12336; *Angew. Chem.* **2017**, *129*, 12505; c) C. Wang, J. Qin, X. Shen, R. Riedel, K. Harms, E. Meggers, *Angew. Chem. Int. Ed.* **2016**, *55*, 685; *Angew. Chem.* **2016**, *128*, 695; d) E. Fava, A. Millet, M. Nakajima, S. Loescher, M. Rueping, *Angew. Chem. Int. Ed.* **2016**, *55*, 6776; *Angew. Chem.* **2016**, *128*, 6888; e) M. Nakajima, E. Fava, S. Loescher, Z. Jiang, M. Rueping, *Angew. Chem. Int. Ed.* **2015**, *54*, 8828; *Angew. Chem.* **2015**, *127*, 8952; f) L. Qi, Y. Chen, *Angew. Chem. Int. Ed.* **2016**, *55*, 13312; *Angew. Chem.* **2016**, *128*, 13506.

[4] a) I. Ghosh, T. Ghosh, J. I. Bardagi, B. König, *Science* **2014**, *346*, 725; b) E. H. Discekici, N. J. Treat, S. O. Poelma, K. M. Mattson, Z. M. Hudson, Y. Luo, C. J. Hawker, J. R. de Alaniz, *Chem. Commun.* **2015**, *51*, 11705; c) M. Majek, U. Faltermeier, B. Dick, R. Pérez-Ruiz, A. Jacobi von Wangelin, *Chem. Eur. J.* **2015**, *21*, 15496; d) I. Ghosh, R. S. Shaikh, B. König, *Angew. Chem. Int. Ed.* **2017**, *56*, 8544; *Angew. Chem.* **2017**, *129*, 8664; e) M. Neumeier, D. Sampedro, M. Májek, V. A. de la Peña O'Shea, A. Jacobi von Wangelin, R. Pérez-Ruiz, *Chem. Eur. J.* **2018**, *24*, 105; f) B. G. McCarthy, R. M. Pearson, C.-H. Lim, S. M. Sartor, N. H. Damrauer, G. M. Miyake, *J. Am. Chem. Soc.* **2018**, *140*, 5088.

[5] a) M. Marchini, G. Bergamini, P. G. Cozzi, P. Ceroni, V. Balzani, *Angew. Chem. Int. Ed.* **2017**, *56*, 12820; *Angew. Chem.* **2017**, *129*, 12996; b) I. Ghosh, J. I. Bardagi, B. König, *Angew. Chem. Int. Ed.* **2017**, *56*, 12822; *Angew. Chem.* **2017**, *129*, 12998.

[6] S. B. Harkins, J. C. Peters, *J. Am. Chem. Soc.* **2005**, *127*, 2030.

[7] a) W. Sattler, M. E. Ener, J. D. Blakemore, A. A. Rachford, P. J. LaBeaume, J. W. Thackeray, J. F. Cameron, J. R. Winkler, H. B. Gray, *J. Am. Chem. Soc.* **2013**, *135*, 10614; b) W. Sattler, L. M. Henling, J. R. Winkler, H. B. Gray, *J. Am. Chem. Soc.* **2015**, *137*, 1198.

[8] L. A. Büldt, X. Guo, A. Prescimone, O. S. Wenger, *Angew. Chem. Int. Ed.* **2016**, *55*, 11247; *Angew. Chem.* **2016**, *128*, 11413.

[9] L. A. Büldt, X. Guo, R. Vogel, A. Prescimone, O. S. Wenger, *J. Am. Chem. Soc.* **2017**, *139*, 985.

[10] a) K. Li, X. Guan, C.-W. Ma, W. Lu, Y. Chen, C.-M. Che, *Chem. Commun.* **2011**, *47*, 9075; b) K. Li, G. Cheng, C. Ma, X. Guan, W.-M. Kwok, Y. Chen, W. Lu, C.-M. Che, *Chem. Sci.* **2013**, *4*, 2630; c) A. Meyer, Y. Unger, A. Poethig, T. Strassner, *Organometallics* **2011**, *30*, 2980; d) K. Li, G. S. M. Tong, Q. Wan, G. Cheng, W.-Y. Tong, W.-H. Ang, W.-L. Kwong, C.-M. Che, *Chem. Sci.* **2016**, *7*, 1653.

[11] CCDC 1417213 and 1845252 contain the supplementary crystallographic data for this paper. These data can be obtained free of charge from The Cambridge Crystallographic Data Centre.

[12] a) T. Hokamp, A. Dewanji, M. Lübbesmeyer, C. Mück-Lichtenfeld, E.-U. Würthwein, A. Studer, *Angew. Chem. Int. Ed.* **2017**, *56*, 13275; *Angew. Chem.* **2017**, 129, 13459; b) M. C. Haibach, B. M. Stoltz, R. H. Grubbs, *Angew. Chem. Int. Ed.* **2017**, *56*, 15123; *Angew. Chem.* **2017**, *129*, 15319.

[13] Y. Unger, D. Meyer, O. Molt, C. Schildknecht, I. Münster, G. Wagenblast, T. Strassner, *Angew. Chem. Int. Ed.* **2010**, *49*, 10214; *Angew. Chem.* **2010**, *122*, 10412.

[14] C. Walling, A. Cioffari, *J. Am. Chem. Soc.* **1972**, *94*, 6059.

Entry for the Table of Contents

COMMUNICATION

Highly reducing triplet excited states of phosphorescent Pt(II) complexes bearing tetradentate bis(phenolate-NHC) ligands having peripheral *N*-carbazolyl groups were observed, with $E([Pt]^{+/*})$ being -2.6 V vs $Cp_2Fe^{+/0}$. These air-stable Pt(II) complexes show intense blue emission and catalyze light-driven reductive coupling of carbonyl compounds and reductive debromination of a variety of unactivated aryl bromides.

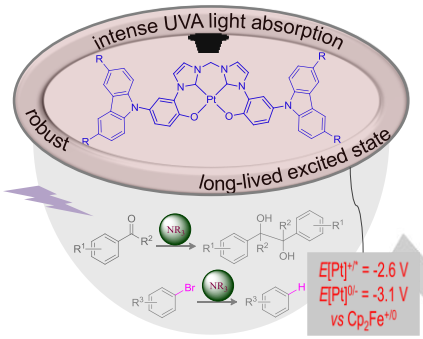

Dr. Kai Li, Qingyun Wan, Dr. Chen Yang, Dr. Xiao-Yong Chang, Dr. Kam-Hung Low, and Prof. Chi-Ming Che*

Page No. – Page No.

Air-Stable Blue Phosphorescent Tetradentate Platinum(II) Complexes as Strong Photo-reductant